

Influence of Electric Field on Orbital Order-Disorder Transition in LaMnO_3

Parthasarathi Mondal,¹ Dipten Bhattacharya,^{1*} and P. Mandal²

¹*Nanostructured Materials Division, Central Glass and Ceramic Research Institute, CSIR,
Kolkata 700032, India*

²*Experimental Condensed Matter Physics, Saha Institute of Nuclear Physics, Kolkata 700064,
India*

We report significant influence of electric field on the orbital order-disorder transition in LaMnO_3 . The transition temperature T_{OO} , thermal hysteresis in the resistivity (ρ) versus temperature (T) data around T_{OO} , and latent heat L associated with the transition decrease with the increase in field. Eventually, at a critical field, L reaches zero. The transition zone, on the other hand, broadens with the increase in field. The states at ordered, disordered, and transition zone are all found to be stable within the time window $\sim 10^{-3}$ to $\sim 10^4$ s.

PACS Nos. 71.70.Ej, 64.60.Cn, 71.30.+h, 71.27.+a

The long range orbital order in LaMnO₃, with ordering of Mn $3d_{3x^2-r^2}$ and $3d_{3y^2-r^2}$ active orbitals within a Mn-O plane and their staggered arrangement across the planes, undergoes an order-disorder transition reversibly at a characteristic transition temperature T_{OO} .¹ The orbital order superstructure originates from cooperative fluctuations of the doubly degenerate Mn $3d e_g^1$ orbitals interacting via Kugel-Khomskii superexchange. This is further aided by cooperative Jahn-Teller distortion of the Mn³⁺O₆ octahedra.²⁻⁴ It is both technologically as well as fundamentally important to find out whether the orbital order-disorder transition can be driven by electric, magnetic or optical stimulations. It has been shown in the past that the long-range *charge order* in the doped systems breaks down under electric, magnetic, and optical stimulations yielding sharp rise in magnetization and/or conductivity together with change in the crystallographic phases.⁵⁻¹³ In spite of such rich background, there is no information about whether or not in pure LaMnO₃ an *orbital order-disorder transition* can be driven by an electric field or optical irradiation. It is all the more important to investigate the nature of the transition – first or higher order.

In this paper, we report that we observe significant influence of electric field on orbital order-disorder transition in LaMnO₃. Using the experimental data, a phase diagram on the current density (J) – temperature (T) plane has been constructed. We found that the latent heat (L) associated with the transition becomes zero at a critical current density $J_C \sim 50$ A/cm². It has also been observed that the transition width broadens continuously as J is increased. The zones in the J - T plane – at well below transition, within the transition region, and at well above the transition – have been characterized by

their resistivity relaxation characteristics together with the resistivity (ρ) versus temperature (T) patterns.

The experiments have been carried out on a high quality single crystal of LaMnO_3 .¹⁴ The measurements of ρ - T and ρ versus time (at a given temperature) patterns under different bias currents were done in linear four-probe configuration. Gold electrodes and wires have been used for the electrical measurements. We have also recorded the differential thermal analysis (DTA) data simultaneously with ρ - T measurements under varying bias current in order to estimate the latent heat of the transition, from the DTA peak around the transition point, as a function of applied current density. We report all the data as a function of the applied current density as the measurements were done by passing different bias current directly through the sample.

In Fig. 1, we show the ρ - T data measured under different bias current. It is quite evident from Fig. 1a inset that the transition temperature T_{OO} decreases under increasing current (or bias voltage). In Fig. 1b, we plot the $d\ln(R/T)/d(1/T)$ versus $1/T$ patterns. The peak marks the T_{OO} in this plot; the height of the peak decreases while the width increases as the bias current increases. The inset of Fig. 1b shows the deviation of the R - T pattern from adiabatic small polaron hopping model $R = R_0 T^\alpha \cdot \exp(\Delta/k_B T)$ ($\alpha = 1$) beyond a certain temperature T^* (marked in the figure by arrow) below T_{OO} . Like T_{OO} , T^* also decreases progressively with the increase in bias current density. The zone confined within T^* and T_{OO} marks the transition zone where both orbital ordered and disordered

phases are expected to coexist and the transport of charge carriers does not follow any model applicable to motion with long range coherence.

An important issue here is the Joule heating of the samples which renders the determination of the electric field driven intrinsic effects difficult. In order to quantify the impact of Joule heating under enhanced bias current (field), we measure the rise in temperature due to heating by attaching a temperature sensor directly onto the sample surface. We found, as expected, that the rise in temperature, as a result of current flow through the sample and sample-current lead junctions, enhances with the enhancement of current density J : from nearly negligible to as high as 100 K for a current range 50 μA – 1 A. We start the current flow through the sample at room temperature and allow the temperature to rise by a certain extent within that range. Once the temperature stabilizes at a particular point above room temperature, we start the measurement. At that point no difference between the furnace (i.e., bath) and actual sample temperature could be noticed.¹⁵ The sample temperature has all along been monitored while recording the ρ - T data. Similar dc current driven measurements on charge ordered compound has earlier been carried and it was found that the impact of Joule heating is minimum.¹¹ In order to quantify the influence of Joule heating, we have compared the dc resistivity pattern with the pattern obtained under pulsed current (4s ‘on’ and 6s ‘off’). Around T_{OO} both the data set are found to be nearly identical establishing negligible role of Joule heating. Moreover, critical examination of the change in the features of transition, such as, broadening of the peak in the DTA pattern, decrease in the hysteresis and jump in ρ - T around the transition, close matching of data between heating and cooling cycles etc

reveals that these are intrinsic field-driven effects.¹⁶ The Joule heating cannot give rise to these changes around T_{OO} .

Figure 2a shows the variation in the latent heat (L) of transition with J . The latent heat is estimated from the area under the peak after subtracting the baseline using an appropriate technique. The peaks appear at the transition points in DTA thermograms both in the heating as well as cooling cycles. With the increase in field, the peaks become broadened (Fig. 2b) with decrease in height. The L is found to decrease gradually with the increase in J and reach zero at $J_C \sim 50$ A/cm² (Fig. 2a). This pattern of variation of L with J is consistent with the variation of the extent of hysteresis (ΔT) in the ρ - T plot around T_{OO} between the heating and cooling runs; ΔT too decreases with the increase in J and vanishes at J_C (inset of Fig. 2a). It is important to mention here that the orbital order-disorder transition even in a very high quality single crystal of LaMnO₃ under nearly zero J is actually a broadened first order transition.¹⁷ No thermodynamic evidence for strictly first order transition has so far been reported. In comparison, compelling thermodynamic evidence for the first order transition has been gathered using local magnetization measurement in the case of vortex lattice melting in high- T_C superconductor. A step-like rise in magnetization could be noticed within a temperature range of ~ 3 mK around the vortex lattice melting line.¹⁸ It has also been shown that disorder can broaden the first order transition.¹⁹ In the present case, of course, the broadening of the transition even under very low field could be because of intrinsic inhomogeneity or disorder due to the presence of orbital domains. Therefore, we compare the latent heat as a function of J only in the sense of noting the relative variation. The nature of the transition actually broadens

progressively and finally becomes broader than the resolution of the instrument. At that point, the isolation of the peak area from the baseline is no longer possible and the estimated L reaches zero. Using a calorimeter of higher sensitivity or a local calorimeter one could possibly resolve the peak.

Using the data of transition temperatures as a function of bias current, obtained both from electrical and calorimetric measurements, we construct a phase diagram on the J - T plane (Fig. 3). The phase diagram marks three regions (i) ordered, (ii) disordered, and (iii) transition. It is clear from the figure that the transition zone broadens progressively with field. Interestingly, the peak broadening, observed in DTA data under enhanced J , covers a rather narrow portion of the T^* - T_{OO} transition zone identified from the electrical resistivity data. It shows that though the electrical measurement senses the onset of transition at T^* , the calorimetric measurement senses the onset at a much higher temperature closer to the thermodynamic T_{OO} . Earlier work²⁰ as well as our experiments²¹ on evolution of crystallographic structure across T^* - T_{OO} , on the contrary, reveals that the structural distortion sets in at $\sim T^*$ itself. The reason behind discrepancy between the onset points identified from the crystallographic and resistivity data and those identified from the calorimetric data is not clear at this moment.

In order to probe further the characteristics of these three regions of the J - T phase diagram, we have measured the relaxation of resistivity. For crossing the boundaries along a constant J line, we selected four points (shown in Fig. 3) with different temperatures. The relaxation measurements were carried out by raising the temperature of

the crystal to the desired point and then applying the requisite current density. We reached the points separately by raising the temperature and field from room temperature and zero-field in order to avoid history effect, if any. The resistivity data were recorded over a time span of ~50ms to 3600s at an interval of ~50ms after stabilizing the sample surface temperature at a given point within less than 0.01 K. We repeated such measurements along other constant J lines too. In Fig. 4, we show the relaxation characteristics observed at points 1, 2, 3, and 4. The characteristics are representative of all the points at which similar relaxation measurements were carried out. We observe virtually *no time dependence of resistivity* corresponding to the points 1, 2, 3, and 4 signifying stability of not only orbital ordered and disordered phases but also of the mixed phase within the transition zone. Therefore, the states at transition zone are not metastable. The transition is thermodynamic and the transition kinetics is not accessible within the laboratory time window $\sim 10^{-3}$ - 10^4 s at all the temperatures. Our probe of evolution of crystallographic structure²¹ shows that O' orthorhombic structure ($c/\sqrt{2} < a < b$; a, b, c are lattice parameters) of the orbital ordered phase evolves into a mixed O' and O orthorhombic phase within the transition zone and finally into a pure O orthorhombic phase ($c/\sqrt{2} \sim a \sim b$) above the transition zone. By taking into consideration the evolution of the structure within the transition zone along with the relaxation data of resistivity, it is possible to conclude that the mixed $O'+O$ phase does not have any temporal fluctuation within the laboratory time window. On the contrary, orbital ordered phase in nanoscale (<20 nm) LaMnO_3 is found to be metastable with 2-4% decay in resistance with time and irreversible order-disorder transition within similar time scale.²² Emergence of transient metastable states with lifetime ($\sim 10^{-3}$ - 10^4 s) comparable to the laboratory time scale has

been observed by Kalisky *et al.*²³ around the vortex solid-solid phase transition as well, in a high- T_C superconductor.

The broadening of the transition width and decrease in the latent heat and hysteresis associated with the transition possibly result from evolution of finer orbital domains as a function of enhanced J . Similar field driven crossover from first to higher order transition has been observed for magnetic transition also and has been attributed to enhanced magnetic inhomogeneity under higher field.²⁴ The orbital ordered phase in pure LaMnO_3 is not a continuum even under zero electric field. It contains domains due to interaction with electronic/lattice defects, strain etc.²⁵ Application of enhanced electric field possibly multiplies the defects or strengthens the strain field and hence its interaction with the orbital order superstructure. This interaction could lead to emergence of even finer orbital domain pattern which, in turn, could give rise to smaller L and hysteresis. Another possibility is the unleashing of charge carriers via $\text{Mn}^{3+} \rightarrow \text{Mn}^{2+} + \text{Mn}^{4+}$ disproportionation reaction under enhanced electric field. Presence of charge carriers could also lead to broadening of transition and decrease in latent heat.²⁶ Study of orbital domain structure under external electric field using spatially resolved resonant x-ray scattering data or charge carrier concentration under enhanced electric field can yield the actual picture of this field driven transition dynamics.

In summary, we observe significant influence of electric field on orbital order-disorder transition in a single crystal of pure LaMnO_3 . The transition temperature, hysteresis, and the latent heat of transition decrease monotonically with the increase in

field; the transition width, on the contrary, increases. Finally, at a critical field, the latent heat becomes zero. The states at the ordered, disordered, and transition zones are all found to be thermodynamically stable within the laboratory time scale.

We acknowledge helpful discussion with R. Nath and A.K. Raychaudhuri. One of the authors (PM, first author) acknowledges financial support from CSIR during this work.

*e-mail: dipten@cgeri.res.in

¹Y. Murakami *et al.*, Phys. Rev. Lett. **81**, 582 (1998).

²K.I. Kugel and D.I. Khomskii, Sov. Phys. JETP **37**, 725 (1973); K.I. Kugel and D.I. Khomskii, Sov. Phys. – Uspekhi **25**, 231 (1982).

³S. Okamoto, S. Ishihara, and S. Maekawa, Phys. Rev. B **65**, 144403 (2002).

⁴E. Pavarini and E. Koch, Phys. Rev. Lett. **104**, 086402 (2010).

⁵Y. Tomioka *et al.*, Phys. Rev. Lett. **74**, 5108 (1995).

⁶A. Asamitsu *et al.*, Nature (London) **388**, 50 (1997).

⁷K. Miyano *et al.*, Phys. Rev. Lett. **78**, 4257 (1997).

⁸V. Kiryukhin *et al.*, Nature (London) **386**, 813 (1997).

⁹S. Yamanouchi, Y. Taguchi, and Y. Tokura, Phys. Rev. Lett. **83**, 5555 (1999).

¹⁰M. Hervieu *et al.*, Phys. Rev. B **60**, R726 (1999).

¹¹C.N.R. Rao *et al.*, Phys. Rev. B **61**, 594 (2000).

¹²K. Hatsuda, T. Kimura, and Y. Tokura, Appl. Phys. Lett. **83**, 3329 (2003).

¹³D. Polli *et al.*, Nat. Mater. **6**, 643 (2007).

¹⁴P. Mandal, B. Bandyopadhyay, and B. Ghosh, Phys. Rev. B **64**, 180405(R) (2001).

¹⁵See supplementary data for more details on how the sample surface temperature was measured. The rise in the sample temperature – even when the furnace is maintained at room temperature – as a function of bias current density is given. The comparison between ρ - T data obtained from continuous dc and pulsed field measurements is also given.

¹⁶Importantly, the experiments have been repeated on several samples of different dimensions. The transition features were found to be reproducible and independent of sample size.

¹⁷J.-S. Zhou and J.B. Goodenough, Phys. Rev. B **68**, 144406 (2003).

¹⁸E. Zeldov *et al.*, Nature (London) **375**, 373 (1995).

¹⁹A. Soibel *et al.*, Nature (London) **406**, 282 (2000); see also, W.K. Kwok *et al.*, Phys. Rev. Lett. **69**, 3370 (1992); Y. Imry and M. Wortis, Phys. Rev. B **19**, 3580 (1979).

²⁰See, for example, G. Maris, V. Volotchaev, and T.T.M. Palstra, New J. Phys. **6**, 153 (2004).

²¹P. Mondal, D. Bhattacharya, J. Ghosh, and S. Mazumder (unpublished).

²²P. Mondal *et al.*, Phys. Rev. B (submitted).

²³B. Kalisky, Y. Bruckental, A. Shaulov, and Y. Yeshurun, Phys. Rev. B **68**, 224515 (2003).

²⁴P. Sarkar *et al.*, Phys. Rev. B **78**, 012415 (2008).

²⁵See, for example, C.S. Nelson *et al.*, Phys. Rev. B **66**, 134412 (2002).

²⁶T. Chatterji, B. Ouladdiaf, P. Mandal, and B. Ghosh, Solid State Commun. **131**, 75 (2004); P. Mondal, D. Bhattacharya, and P. Choudhury, arXiv:0912.5432 (2009).

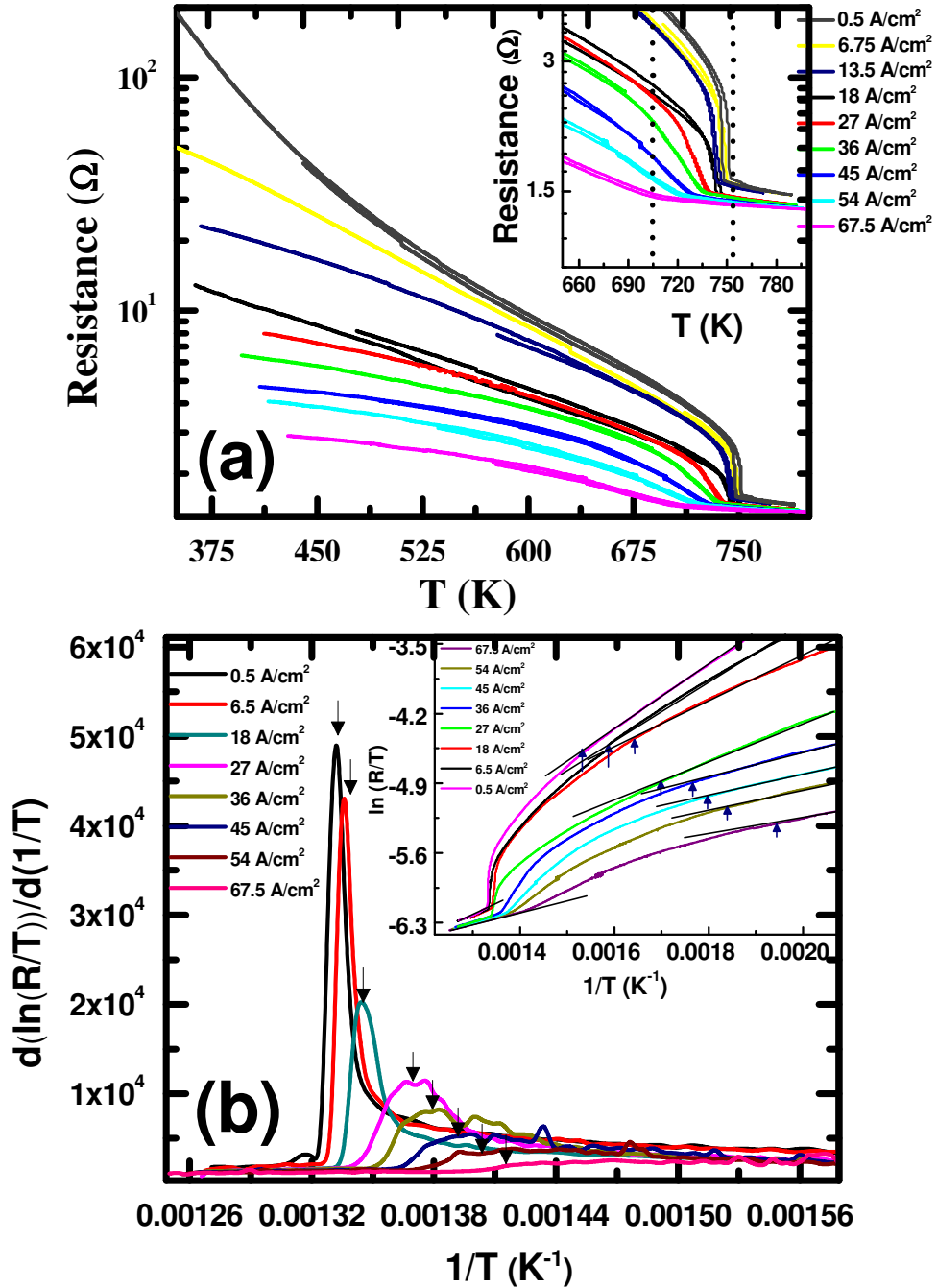


Fig. 1. (color online) (a) The resistance (R) versus temperature (T) plot under different bias current at above room temperature showing the variation in T_{00} with the bias current density; inset: the region around T_{00} is blown up; (b) The $d(\ln(R/T))/d(1/T)$ versus $1/T$ plots for different bias current density obtained from the resistance (R) versus temperature (T) data; the temperature corresponding to the peak is the T_{00} while in inset the onset of the transition (T^*) is marked by arrow. T^* perhaps also marks the orbital solid to glass crossover point. In the orbital solid phase, the small polaron hopping conduction model remains valid and hence the linearity in $\ln(R/T)$ versus $1/T$ plot prevails. In the orbital glass phase, on the other hand, small polaron hopping model fails signifying a disordered or short-range order.

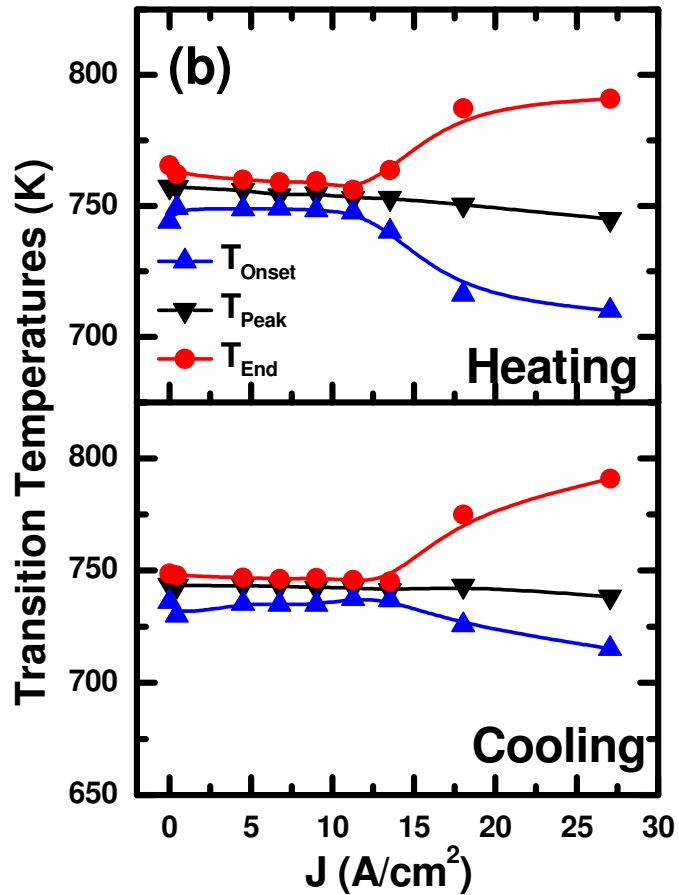
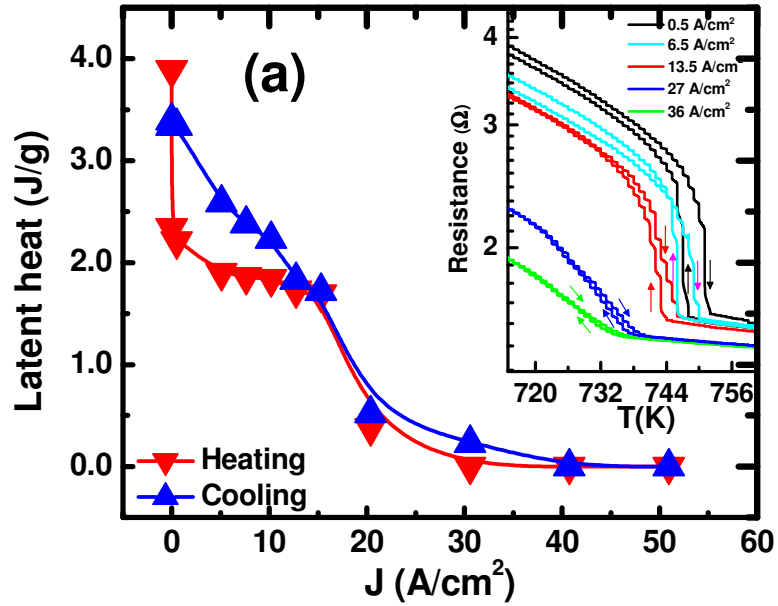


Fig. 2. (color online) (a) The variation of latent heat – estimated from the area under the peak observed in DTA thermogram near the orbital order-disorder transition point – with bias current density (J); inset shows how the extent of hysteresis decreases with the increase in bias current density (b) variation of the transition temperatures (noted from DTA thermograms) with J ; obviously the transition width increases with J .

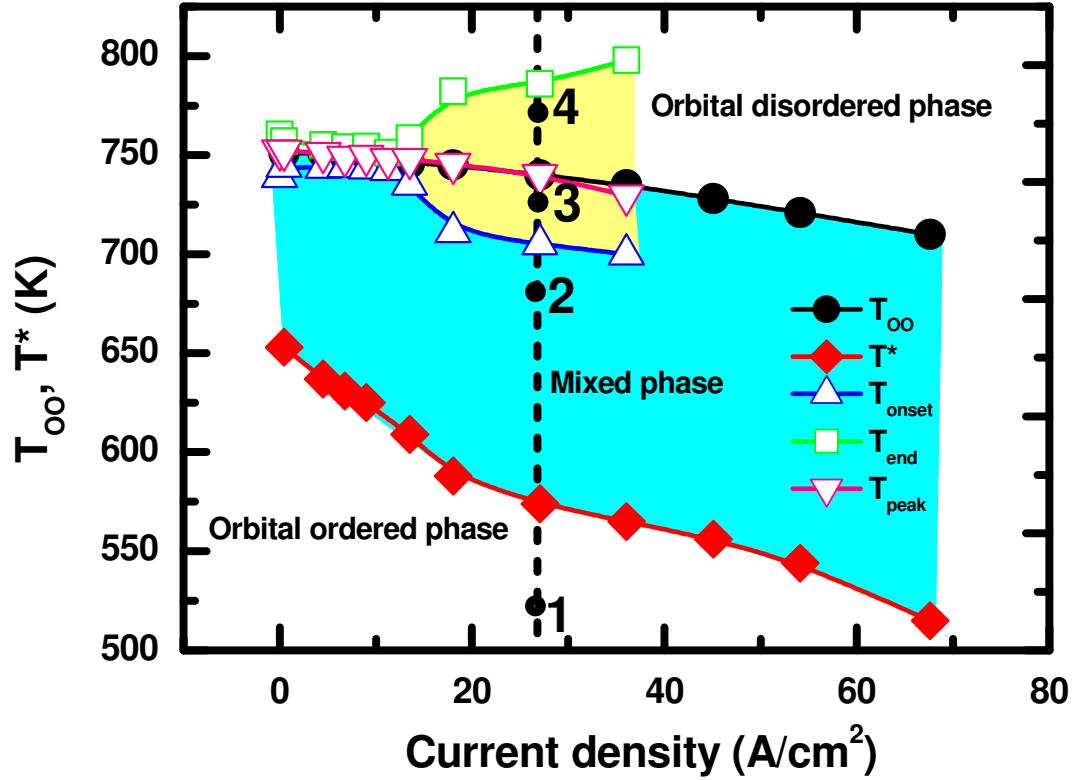


Fig. 3. (color online) The phase diagram of electric field driven orbital order-disorder transition on the J - T plane; the transition width increases with the increase in J . The peak width of the DTA data has been superimposed on the phase diagram. It shows that the DTA peak width is quite smaller in comparison to the transition width identified from the electrical resistivity data. The points at which the data of relaxation of resistivity have been presented in Fig. 4 are shown as 1, 2, 3, and 4.

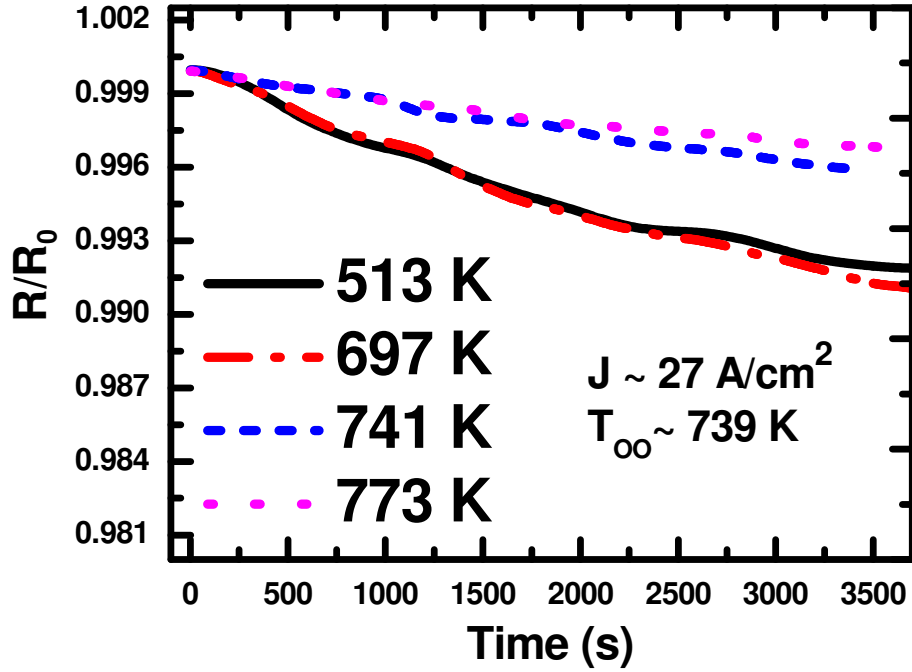


Fig. 4. (color online) A representative plot of time dependence of normalized electrical resistance at different temperatures under a bias current density $\sim 27 \text{ A/cm}^2$. The temperatures and the bias current are chosen in such a way so that different regions of the phase diagram – ordered, disordered, and transition – can be accessed. The extent of relaxation appears to be negligible in all the cases indicating stability of the phases. On the contrary, 2-4% decay in resistance could be noticed²² in the case of metastable orbital ordered phase in nanoscale ($\leq 20 \text{ nm}$) LaMnO_3 .

Supplementary Data on the Impact of Joule Heating

The measurement of resistance versus temperature pattern of the single crystal of LaMnO_3 has been carried out using linear four-probe configuration in constant dc current mode. The contacts were made by gold paste and wires. The contact resistance was measured to vary within 30-85 $\text{m}\Omega/\text{mm}^2$. Because of Joule heating, the rise in temperature of the sample was from nearly negligible to ~ 100 K at room temperature. We provide here the bias current density (J) and corresponding temperature rise (Table S1). The rise in temperature was measured by attaching the sensor directly onto the surface of the sample (Fig. S1). The sample temperature, thus measured, stabilizes at a particular value for a particular bias current density while the furnace (i.e., bath) is maintained at room temperature. After stabilization of the sample temperature, the furnace power supply is turned on. Initially the sample temperature remains nearly fixed and the furnace temperature increases. The temperature difference between the furnace and sample gradually decreases. Eventually they become identical signaling a state of equilibrium between the sample and the furnace. The sample, at any given time thereafter, is heated both by the furnace as well as by Joule heating because of current flow. When the sample reaches equilibrium with the furnace, the impact of Joule heating should be minimum. Otherwise, the sample temperature would have always been higher than the furnace temperature. With the rise in temperature, the sample resistance drops down enormously and hence the extent of Joule heating. Therefore, around the orbital order-disorder transition point T_{OO} (700-750 K), the impact of Joule heating turns out to be quite less. The sample temperature, thus measured, gives the true temperature of the sample as the sample is quite homogeneous.

Fig. S1. The measurement arrangement

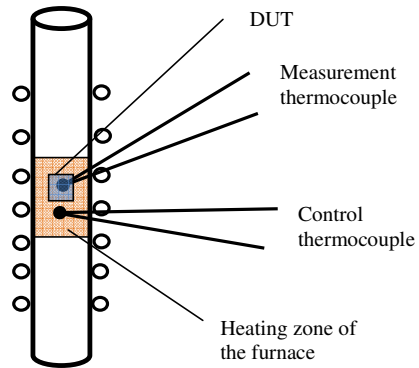


Table S1. List of sample temperature – measured by a sensor attached to the sample surface – under a certain bias current density

| Bias Current Density (A/cm^2) | Rise in Sample Surface Temperature* when the Furnace is maintained at Room Temperature |
|---|--|
| 0.5 | 0 |
| 5.0 | 36.0 |
| 9.0 | 40.0 |
| 36.0 | 65.0 |
| 45.0 | 86.0 |
| 67.5 | 97.0 |

*The sample surface temperature is noted after it stabilizes at a particular value following the initial rise

We have also measured the resistance of the sample by using pulsed current mode (a section of the pulse is shown in Fig. S2). We recorded the voltage (V) – current (I) characteristics at different temperatures across 77-700 K. We can construct the resistance versus temperature plot for a fixed bias current density using the V - I characteristics at different temperatures. In Fig. S3, we show two such representative resistance versus temperature plots. It shows that data obtained from pulsed and continuous dc measurements match with each other quite well. This also proves that the impact of Joule heating is not significant.

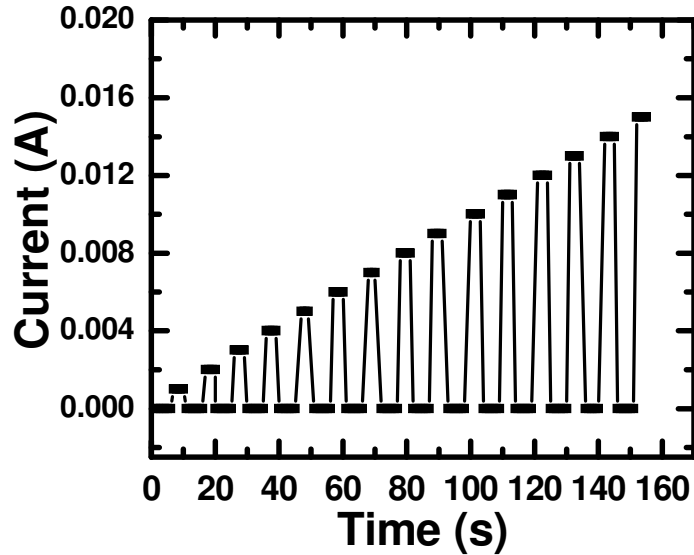


Fig. S2. A section of the pulsed current pattern used to measure the voltage-current characteristics at different temperature. The pulse consists of 4s ‘on’ and 6s ‘off’ sequence.

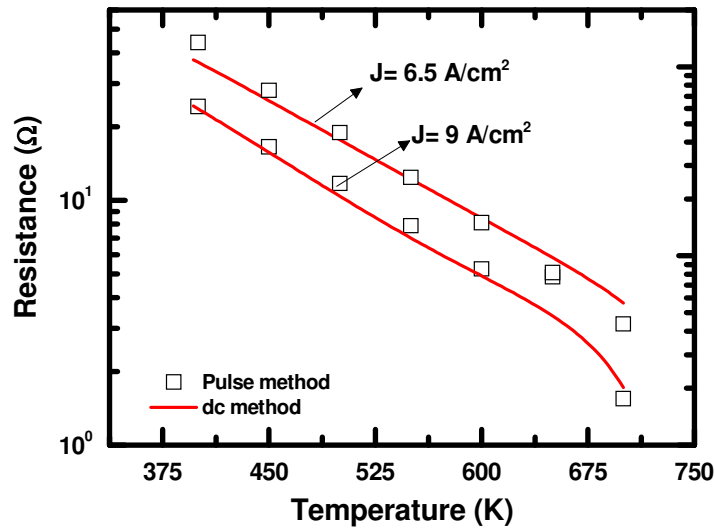


Fig. S3. Two representative resistance versus temperature patterns obtained from pulsed and continuous dc current modes. The matching of the data is quite well signifying lesser impact of Joule heating during continuous dc mode measurement.

Beside these, we point out that the critical features of the transition – transition width, latent heat, hysteresis associated with the transition etc. – vary significantly under higher bias current density i.e., electric field. These changes are reflection of intrinsic electric field driven effect on orbital order-disorder transition. These changes cannot arise because of Joule heating alone. Measurements have been repeated on several pieces of crystals of different dimensions. These features were found to be reproducible and independent of crystal size.